DYNAMIC FRACTURE TOUGHNESS IN MIXED MODE OF A MAGNESIUM ALLOY

NEVIERE R. TOLBA B. PLUVINAGE G.*

A method to obtain intrinsic failure curve in dynamic loading condition is presented. It consists of thin tube with an arbitrary oriented crack which is submitted to a pressure pulse generated by a shock wave. This tube is inserted between the incident and the transmitted rod of a split Hopkinson bar. An example of a dynamic intrinsic failure curve of a Magnesium alloy is presented and discussed.

INTRODUCTION

Magnesium is used under multiple forms : as an alloying element in aluminium alloys, in nodularisation of iron, desulfuration of steel, chemical and reduction processes, cathodic protection. Magnesium alloys can be produced also in all wrought and cast forms, but this use in 1985 represented 45.000 metric tons over a total of primary consumption in Western World of 226.000 tons of magnesium.

Castability, productivity and versability are in favour of pressure die casting with magnesium alloys. The widespread acceptance of light metal castings in cars would mean that magnesium alloys can be used for many parts, if some progress can be made on corrosion resistance, deep drawing and mechanical properties.

Because of its hexagonal structure, magnesium is relatively sensitive to strain rate. Experimental results given by Davies and Hunter / 1 / and Senseney et al / 2 / indicate that the strain rate sensitivity coefficient μ_{12} of magnesium is in the range of 2-4.

* Laboratoire de Fiabilité Mécanique - Université de Metz - FRANCE

This coefficient is defined by the following expression :

$$\mu_{12} = \frac{\tau_2 - \tau_1}{\ln(\gamma_2 / \gamma_1)} \qquad (1)$$

where τ_2 and τ_1 are the respective values of shearing stress obtained in torsion tests at constant strain-rates γ_2 and γ_1 .

Very few data on the fracture toughness of magnesium exist in literature / 3 / / 4 / and there is no data on dynamic fracture toughness i.e at a value of stress intensity factor rate $\dot{K}$ up to 10^6 MPa$\sqrt{m}$/s. A frequently encountered problem in engineering applications of fracture mechanics is the mixed mode loading of a crack subjected to biaxial tension. To obtain a conservative estimate of the load required for crack initiation it is only necessary in many cases to perform calculations according to mode I type of loading. This underestimate the fail safe load and holds very well for isotropic media.
In this paper, a method for determination of mixed mode dynamic fracture toughness of magnesium alloy tubes is described and dynamic intrinsic curve of failure of this material is presented.

MATERIAL AND EXPERIMENTAL DEVICE

Dynamic fracture toughness tests have been performed on an aluminium-magnesium alloy GA3Z1 containing 3 % aluminium and 1 % zinc. The mechanical properties of this alloy are presented table I.

	Re (MPa)	Rm(MPa)
$\dot{\varepsilon} = 10^{-3}.s^{-1}$	143,5 MPa	220,7 MPa
$\dot{\varepsilon} = 10^{3}.s^{-1}$	200 MPa	290 MPa

Table I

Static tests are performed at low strain rate ($\dot{\varepsilon} = 10^{-3} s^{-1}$) while dynamic tests ($\dot{\varepsilon} = 10^{+3}\ s^{-1}$) are performed using a split Hopkinson pressure bar. The stress-strain curves in the two cases are shown in figure 1.
The material was obtained as round bars of 30 mm diameter. Wedge loading CT (WLCT) samples of 20 mm thickness and tube of 22 mm inner diameter, 1 mm thickness and 25 mm length were issued of these bars. The geometry and the details of the slots of these two kind of samples is described in figures 2 and 3.
The depth c, the angle β with the longitudinal direction the length 2a of the slots in tube samples are given in table II.

β°	0	15	30	45	60
2a (mm)	6,75	6	4,75	4,5	3,75
c (mm)	0,6	0,5	0,5	0,5	0,5

Table II

The WLCT samples were fatigue precraked with ratio a/W = 0,5. Dynamic fracture toughness was obtained using a split Hopkinson pressure bar.

The dynamic loading of the WLCT is given by a stress wave produced by the impact of a projectile on the incident road of a split Hopkinson pressure bar device. This method is shown schematicaly in Figure 4 and described in reference / 5 /.
The recorded transmitted pulse provides the critical applied load for fracture F_C. The friction between the wedge and the specimen has to be taken into account. The relation between critical load P_C and the applied load F_C is given by :

$$P_C = F_C \cdot \frac{1}{2 \operatorname{tg} \left(\frac{\delta}{2} + \lambda \right)} \qquad (2)$$

δ is the wedge angle, λ = arctg μ is the friction coefficient. For magnesium-steel contact a value of μ = 0,17 has been measured bythe authors according to Klepaczko method described in reference / 16 /.

The small size of the specimen and the relatively long time for fracture (20 μ s), compared to the travel time of the wave (150 μs), leads to the conclusion that the dynamic applied stress intensity factor is only slightly different to the static applied stress intensity factor and the quasistatic assumption can be used to calculate the critical stress intensity factor (5).

A further development of the dynamic fracture toughness in mode I was achieved to procedure mixed mode of rupture. It consists of the same split Hopkinson bar apparatus, but the specimen is now a tube, the interior of which is filled with oil. A pressure pulse from the incident rod builds up an hydrostatic pressure in the tube. The device gives necessary fluid tightness using "O" rings between bar and device (1) and tube and device (2) as can be seen in figure 5.

The free ends of the tube are in contact with teflon rings (3) in

order to prevent tube buckling. The oil is filled by the holes n° 4 in figure 5.

This method is similar to the one used by Ohlson / 6 / / 7 /.The transmitted wave produced by impact is registred with strain gages glued on the rod. The electrical signal is amplified and recorded on a digital oscilloscope. A typical example of the registred transmitted wave can be seen in figure 6. Due to the fact that oil is not absolutely incompressible, radial inertia causes transversal waves which interfer with the signal. The critical pressure is then a average value.

ANALYSIS OF THE RESULT

The inclined crack in such a tube is submitted to a biaxial loading. The pressure provides membrane stress, but since the symmetry of the tube is disturbed by the crack, bending stress must be taken into account. In addition the loading rate being relatively high, time to fracture (40-80 μs), and fracture process can be considered as dynamic. This will mean that the mechanical properties are modified by strain rate. As previously mentionned the total travel time of the wave is relatively long compared to travel time in specimen and the inertial effect on stress history can be neglected.
This procedure is called quasi-static approximation and can be used if the following criteria is respected.

$$\frac{C_\ell \cdot T_r}{2a} \gg 10 \qquad (3)$$

This is the case in our tests. (C_ℓ celerity of wave, T_r time to rupture, 2a crack length)

The defect in the tube is a surface defect, but, as the tube is relatively thin (1 mm), the ligament between the bottom of the defect and the inner surface is easily plastified. In this case the surface defect can be considered as a "through the thickness" defect. This procedure is usualy used for recategorisation of defects. Althougt, the tube fails in the ductile range, the analysis is based on an apparent fracture toughness K_c.

This apparent fracture toughness is defined as the value of the equivalent elastic and critical stress intensity factor multiplied by a plasticity-Irwin type correction ρ_o.

$$K_c^* = K_{Ie}^c \cdot \sqrt{\rho_o}$$

The stress intensity solutions for an arbitrary oriented "trough the thickness" crack in a long cylindrical shell have been obtained by Lakshminarayana and Murthy / 8 / / 9 / using a analytical numerical procedure.

The method of analysis involved obtains series solutions to the governing thin shell equation :

$$\nabla^4 F + 8i.\alpha^2 . \frac{\partial^2 F}{\partial x^2} = 0 \qquad (5)$$

where $\alpha^2 = (a^2/8Rt) \; / \; [\, 12\,(1 - \nu^2)\,]^{\frac{1}{2}}$ with R radius of curvature of the shell, t the thickness and a half the crack length.

The solutions of equation (5) keep the following criteria
- periodicity of solutions
- symmetry considerations
- stress and displacement vanish when $x \rightarrow \infty$

This method leads to a stress function $\phi\,(r,\theta)$ and real displacement $W(r,\theta)$ of the form :

$$\phi = \phi_0 + \phi_1 r^{\frac{1}{2}} \cos\frac{\theta}{2} + \phi_2 r\cos\theta + \phi_3 r^{3/2} \cos\frac{\theta}{2} + \phi_4 r^{3/2} \cos\frac{3\theta}{2}$$

$$+ \phi_5 r^{\frac{1}{2}} \sin\frac{\theta}{2} + \phi_6 r \sin\theta + \phi_7 r^{3/2} \sin\frac{\theta}{2} + \phi_8 r^{3/2} \sin\frac{3\theta}{2} + O(r^2)$$

$$W = W_0 + W_1 r^{\frac{1}{2}} \cos\frac{\theta}{2} + W_2 r \cos\theta + W_3 r^{3/2} \cos\frac{\theta}{2} + W_4 r^{3/2} \cos\frac{3\theta}{2}$$

$$+ W_5 r^{\frac{1}{2}} \sin\frac{\theta}{2} + W_6 r \sin\theta + W_7 r^{3/2} \sin\frac{\theta}{2} + W_8 r^{3/2} \sin\frac{3\theta}{2} + O(r^2)$$

The ϕ_i, W_i functions are numerically tabulated and the stress intensity factors in mode I and II are given by the superposition of the membrane and bending stress intensity factors :

$$K_I^{(m)} = 3\,(\phi_3 + \phi_4) \; / \; 2\sqrt{2}$$

$$K_{II}^{(m)} = (\phi_7 + 3\,\phi_8) \; / \; 2\sqrt{2}$$

$$K_I^{(b)} = 3\,[\,3\,(1 - \nu) W_4 - (5 + 3\nu) W_3\,] \; / \; [\,24\,(1 - \nu^2)\,]^{\frac{1}{2}}$$

$$K_{II}^{(b)} = 3\,(\nu - 1).[\,W_7 + 3W_8\,] / [\,24\,(1 - \nu^2)\,]^{\frac{1}{2}}$$

Here the subscripts m or b refers to membrane or bending stress and the subscripts I for II refers to mode I or II. In the original paper of Lakshminarayana and Murthy, the non-dimensional stress intensity factors with respect to $\sigma\sqrt{a}$ are given as a graph function of the β angle and for different values of the parameter. These non-dimensional stress intensity factors are called respectively Cm_I, Cm_{II}, Cb_I, and Cb_{II} the subscripts having the same meaning as previously.

PRESENTATION OF RESULTS

A serie of tests with five values of have been performed in order to build an intrinsec failure curve $K_{IIe}/K^*_c = f(K_{Ie}/K^*_c)$ where K_{Ie} and K_{IIe} are the apparent fracture toughness in mode I and mode II and K_c is the apparent fracture toughness measured with the same test but with $\beta = 0°$.

The results are presented in table III, where are listed for the different β values : the membrane stress σ_m, the halfcrack length a and the coefficients f_I and f_{II} which are defined by the following relation-ship :

$$\frac{K_{Ie}}{\sigma_m \sqrt{a}} = f_I \quad , \quad \frac{K_{IIe}}{\sigma_m \sqrt{a}} = f_{II} \qquad (8)$$

These coefficients include Irwin's plasticity correction ρ_o, finite length correction C_e according to / 10 /, and Lakshminarayana bending and membrane coefficients :

$$f_I = \sqrt{\rho_o} \cdot C_e \cdot (C_{mI} + C_{bII})$$
$$f_{II} = \sqrt{\rho_o} \cdot C_e \quad (C_{mII} + C_{bII}) \qquad (9)$$

The intrinsic failure curve is presented in Figure 7. In the same figure is presented an other failure curve relative to aluminium alloy A5G for comparaison.

For an isotropic and brittle material in which the failure in mixed mode is governed by the SIH criteria / 14 /, the intrinsic failure curve can be described by the following relationship :

$$(K_I / K_{Ic})^2 + (K_{II} / K_{Ic})^2 = 1$$

The effects of anisotropy, geometry and ductility effects modifies the shape of intrinsic failure curve which then can be more generally described by :

$$(K_{Ie} / K^*_c)^u + (K_{II} / K^*_c)^v = 1$$

where u and v are empirical coefficients, K_c is the apparent fracture toughness and K_{Ie}, K_{IIe} are the equivalent elastic stress intensity factors. We notice that the intrinsic failure curve of the magnesium alloy shows a small influence of the K_{Ie} value in a large portion of the curve. This shape is inherent to anisotropic materials and has been observed by Jodin / 15 /.

MAGNESIUM ALLOY								
N°	β	σ_m	2a	2c	f_I	f_{II}	K_{Ie}	K_{IIe}
		MPa	mm	mm			MPa$\sqrt{m}$	MPa$\sqrt{m}$
1-00-G	0°	116,6	6,75	0,6	3,375	0	32,3	0
2-00-G		118,3	6,75	0,6	3,375	0	32,8	0
1-15-G	15°	132,8	6	0,5	3,042	0,5265	31,3	5,4
2-15-G		116,6	6	0,5	3,042	0,5265	27,5	4,8
1-30-G	30°	124,7	4,75	0,5	2,035	0,6050	17,5	6,1
2-30-6		120,4	4,75	0,5	2,035	0,6050	16,9	5,9
1-45-G	45°	142,8	4,5	0,5	0,9975	0,63	9,6	6,0
1-60-G	60°	149,1	3,75	0,5	0,4613	0,5125	4,2	4,7
2-60-G		146,4	3,75	0,5	0,4613	0,5125	4,1	4,6

Table III

DISCUSSION

As mentioned previously, the fracture toughness data of magnesium alloys are very scarce. Hickerson / 4 / gave a value of K_c = 48,6 MPa m for GA3Z1 alloy using a 4 mm CT sample, using a 20 mm thickness WLCT sample we have gota static value K_{Ic} = 20,33 MPa m and dynamic value of K_{Ic} = 18,50 MPa m. Using a tube of 1 mm thick an apparent dynamic fracture toughness K_c = 32,5 MPa m is obtained. This value is in the same order of magnitude as K_{Ic} or K_c values in respect to the increasing loading rate and decreasing thickness
These parameters affect the fracture toughness in an opposite manner : high loading rate decreases the fracture toughness, while decreasing thickness increases the fracture toughness.

The concept of intrinsec failure curve is a particular form of Mohr-Caquot criteria / 11 / / 12 /. A modification of this criteria using a description of normal and shearing stresses based on the values of the mode I and mode II stress intensity factors has been proposed by Mandel / 13 /.

A fractography investigation of the failure surface of magnesium alloy WLCT sample indicates that a typical fibrous fracture appears (figure 8). For comparison an aluminium alloy intrinsic curve is shown in figure 7. The aluminium alloy (cubic centered cristallographic system) is generally considered as an isotropic material, which is not the case of magnesium alloy (hexagonal cristallographic system). The mutual effect of approximatively orthogonal to the principal maximum stress direction. The geometrical influence including mode III friction effects gives an underestimation of K_{IIe} values for β angle higher than 45°. This phenomena appears on the two intrinsic failure curves.

CONCLUSION

Dynamic fracture toughness of a magnesium alloy, in mixed mode of loading has been measured using a split Hopkinson pressure bar apparatus and thin tubes.
The intrinsec failure curve presents a large portion which is independent of the mode I equivalent elastic stress intensity factor. This phenomenon can be explain by the orthotropy and the ductility of the material.

LIST OF SYMBOLS

μ_{12}	strain rate sensitivity coefficient
$\sigma_1 \sigma_2$	shearing stresses in torsion test at constant shearing strain rates
$\dot{\gamma}_1 \dot{\gamma}_2$	shearing strain rates
$\dot{K}$	stress intensity factor rate
$\dot{\varepsilon}$	strain rate
Re	yield stress
Rm	ultime stress
β	crack angle with longitudinal direction of the tube
a	half crack length
c	crack depth

F_c	critical applied load (WLCT)
P_c	critical load (WLCT)
δ	wedge angle
λ	friction coefficient
$C\ell$	celerety of the wave
T_r	time to rupture
K_c^*	apparent fracture toughness
K_{1e}^c	critical equivalent elastic stress intensity factor (mode I)
ρ_o	Irwin plasticity coefficient
ν	poisson's coefficient
$K_I^{(m)}$	membrane, mode I stress intensity factor
$K_{II}^{(m)}$	membrane, mode II stress intensity factor
$K_I^{(b)}$	bending, mode I stress intensity factor
$K_{II}^{(m)}$	bending, mode II stress intensity factor
$\overline{\sigma m}$	membrane stress
C_{mI}	non dimensional stress intensity factors (subscripts refers to membrane, I to mode I)
C_{mII}	(subscripts refers to membrane, to mode II)
C_{bI}	(subscripts refers to bending, to mode I)
C_{bII}	(subscripts refers to bending, to mode II)
$f_{I,II}$	coefficient stress intensity factors correction coefficients
Ce	finite length correction

Bibliographie

1) DAVIES E.D.H. and HUNTER S.C
Journal of Mechanical Physic Solids 11-155.79 (1963)

2) SENSENY P.S, DUFFY J and HAWLEY R.H
Journal of Applied Mechanics 45-60.6 (1978)

3) POOK L.P and GREENAN A.F
Engineering Fracture Mechanics 5 p. 935-946 (1978)

4) HICKERSON J.P
Engineering Fracture Mechanics 9 p. 75-85 (1977)

5) PLUVINAGE G. and MARANDET
Proceeding of ICF6 New Dehli India (1984)

6) OHLSON N.G
"Determination of crack initiation at high strain rates"
Insitute of physics conference série n° 47 Chap. 2, p. 215 (1979)

7) OHLSON N.G
"The effect of strain history under dynamic loading"
Shock waves and high strain rate phenomena chap. 12, p. 193 à 203
Ed. M. Meyers ; L. Murr
Plenum publishing corp. New York

8) LASHKMINARAYANA H. and MURTHY V.V
"On stresses around an arbitrarily oriented crack in a cylindrical shell"
International Journal of Fracture, Vol. 12, n° 4 (1976)

9) LASHKMINARAYANA H. and MURTHY V.V
"On an analytical numerical procedure for the analysis of cylindrical shells with arbitrarily oriented cracks"
International Journal of Fracture, Vol. 19, n° 4 (1982)

10) ROOKE D.P. and CARTWRIGHT P.J
"Stress intensity factors"
H.M. Stationnary Office, p. 298

11) MOHR R.
Abh. aus dem Gebiete des Techn. Mechanik, 2ème Ed. p. 192, ERNST and SOHN Berlin (1914)

12) CAQUOT A.
Compte-rendus du 4ème Congrès International de Mécanique Appliquée, Cambridge (1935)

13) MANDEL J.
"Contraintes à l'extrémité d'une fissure en élasticité plane"
Séminaire de l'Ecole Polytechnique (1968)

14) ERDOGAN F. and SIH G.C
"On the crack extension in plane under loading and transverse shear"
Journal of Basic Engineering Trans ASME p. 519-527 (1963)

15) JODIN P.
"Contribution à l'étude des modes mixtes de rupture"
Thèse, Université de Metz (1984)

16) KLEPACZKO J.R
"Determination of the critical value of J-Integral at high loading rate using the wedge-loaded specimen"
Journal of testing and evaluation, November 1985 p. 441-445

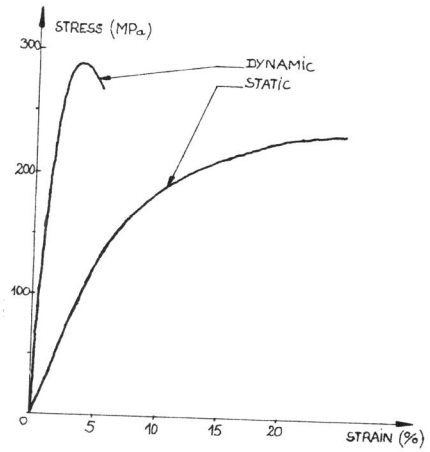

Figure 1 : Stress-strain déflection curves for dynamic and static loading rates

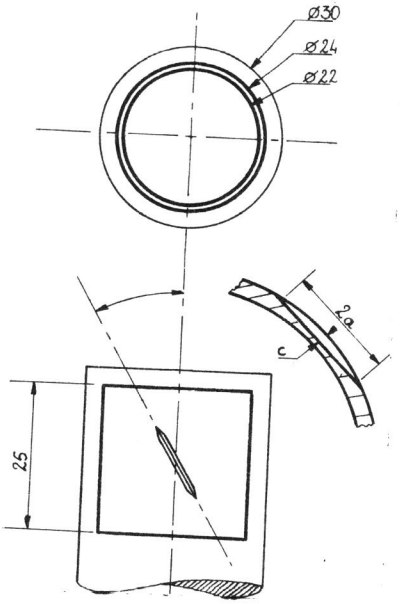

Figure 2 : Thin tube sample

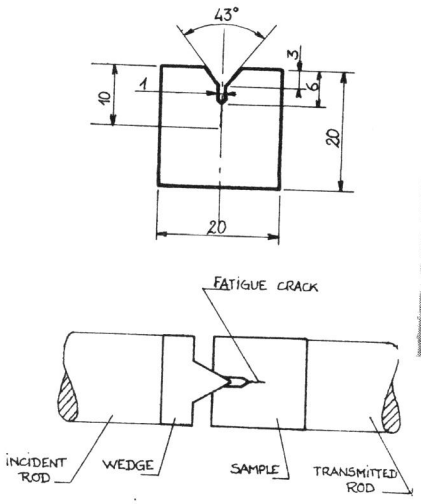

Figure 3 : WLCT 20 SAMPLE

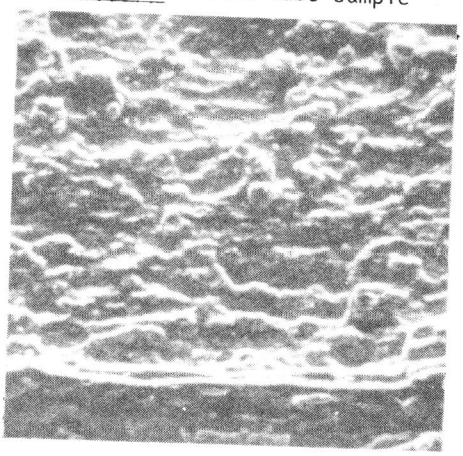

Figure 8 : Fractography of dynamically loaded mg specimen (WLCT)

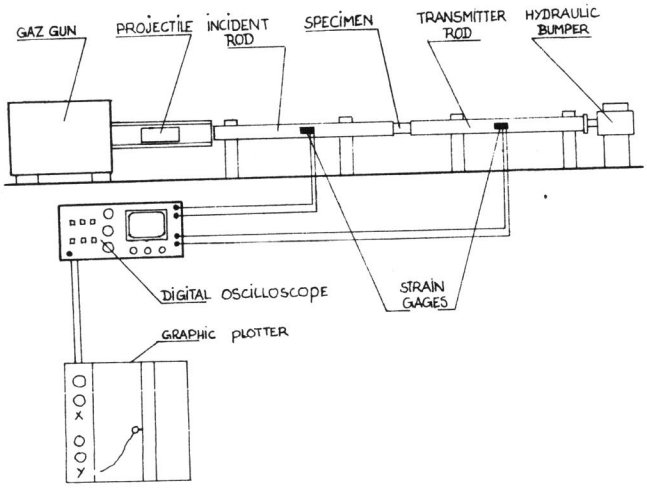

Figure 4 : Split Hopkinson pressure bar

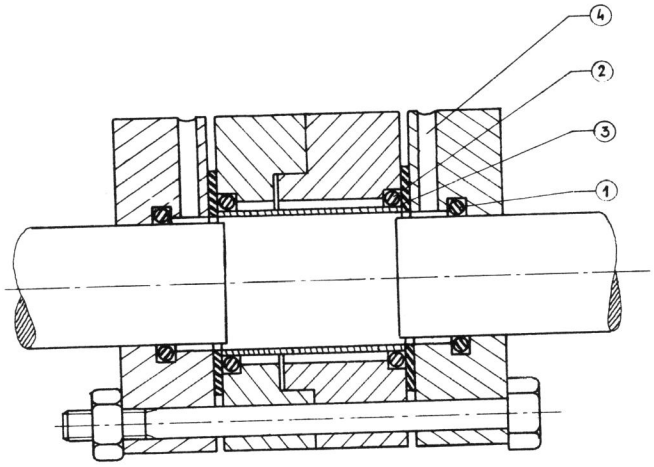

Figure 5 : Pressure chamber

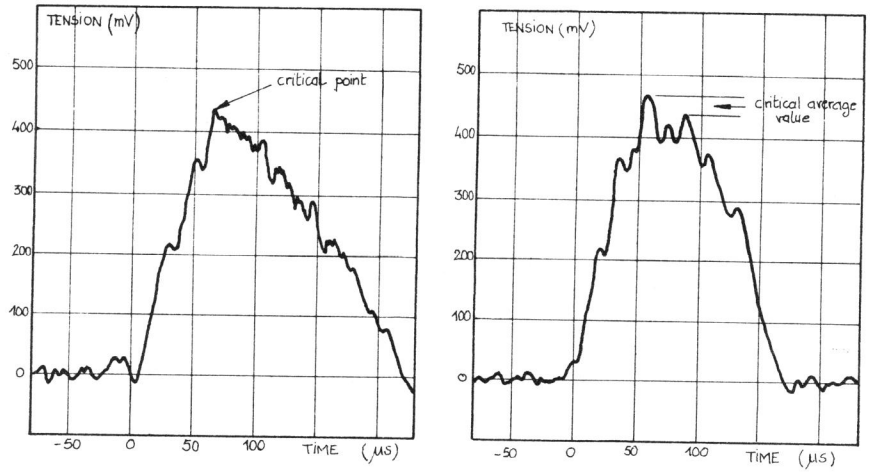

Figure 6 : Typical exemples of registered transmitted wave
a) the critical value of the pressure can be easily determined
b) Inertial effects lead to an average value

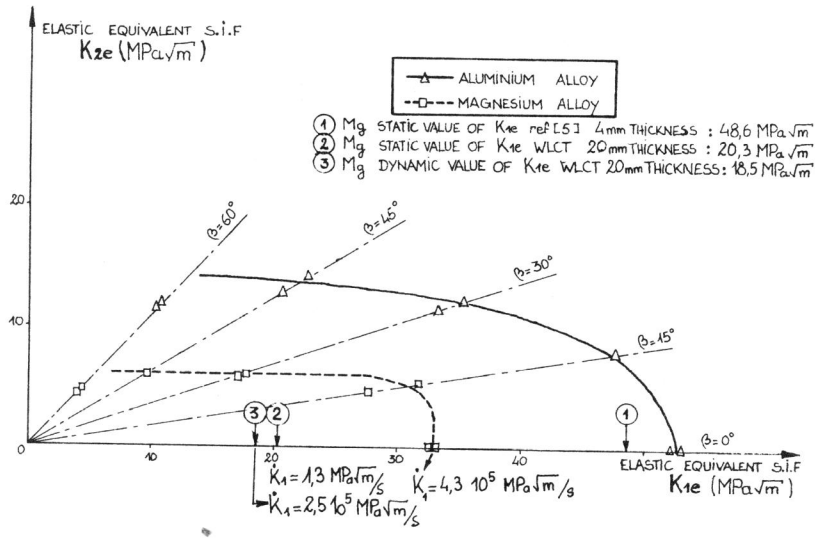

Figure 7 : Intrinsic failure curve for Magnesium and aluminium alloys